# 3D Simulation and Validation of RCL-E and MER Rover Types Mobility

**A. Gibbesch[(1)], B. Schäfer[(1)], S. Michaud[(2)]**

[(1)]*DLR - German Aerospace Center*
*Institute of Robotics and Mechatronics*
*D-82230 Weßling, Germany*
*andreas.gibbesch@dlr.de, bernd.schaefer@dlr.de*

[(2)]*Contraves Space AG*
*Schaffhauserstr. 580*
*CH-8052 Zürich, Switzerland*
*stephane.michaud@oerlikon.com*

## INTRODUCTION

Within the ESA Aurora programme for planetary exploration, powerful rovers (primarily the ExoMars rover for Mars exploration) with different capabilities will be developed. Since mobility has to be guaranteed for these rovers in rough and unknown terrain with almost fully autonomous motion planning, they need extensive all-terrain locomotion capabilities. In order to achieve a successful mission and to enhance the overall rover mobility performance, efficient modelling and simulation tools are required that predominantly cope with the wheel-soil interaction and which regard the overall rover-chassis set-up based on a multibody system (MBS) approach including all the various kinematic suspension and wheel mobility concepts for different rover types. In the field of terramechanics the interaction of a vehicle's wheels on soft soil is investigated. Within the approach of multibody simulation of off-road vehicles the terramechanical wheel-soil module is integrated into the vehicle MBS model with a standard tyre interface. Appropriate quasi-static soil parameters coupled with dynamic- and velocity-dependent soil parameters result in a dynamic MBS model based on the rheological soil model [1].

Very recently, ESA had contracted the Mars RCET study (Rover Chassis Evaluation Tool), resulting in both software and hardware elements that will be interwoven to result in a user-friendly environment. However, in this study mobility investigations have been conducted on a more or less static or quasi-static basis. Our approach proceeds much further, i.e. it is based on MBS models with strongly integrated coupling between vehicle and wheel-soil dynamics. In this regard it is possible to simulate the full dynamic behaviour of the overall rover chassis suspension system interacting with various soil characteristics, whatever level of detail in MBS modelling may be required. With respect to mobility analysis, the necessary scenarios to be investigated are: wheel slippage, slope stability (rover tip over) and slope performance considering slip on soft soil.

Complementary to the RCET study results simulation studies based upon our MBS approach are conducted. Therefore, two types of rovers will be investigated: the NASA MER rover and a modified ESA RCL-E rover which is comparable to the MER rover. The main modifications of the RCL-E rover are the use of MER wheels and the reduction of payload to obtain a similar total weight of the rovers.

The simulation scenarios have been taken from those defined within the RCET study: measurements from two different testbeds are available, one dedicated to a single-wheel characterisation and another one for the rover system-level locomotion performance that allows proper evaluation and validation of the simulation applications. MBS based simulations are run on soft and hard ground whereby wheel longitudinal slip modelling on soft ground is essential for performance evaluation especially slope performance when considering driveaway on steep slopes that are on the verge of static stability. In particular, highly critical situations even as far as the immobility of the rover in former missions showed that mobility performance is sometimes critical even on plane ground without obstacles but very loose, non-cohesive soil which frequently leads to severe slipping conditions.

## MBS MODELLING OF TERRAMECHANICS

Analytical simulation models are based upon the methods of Bekker and Wong [2, 3] gaining the parameters for tyre-sinkage behaviour from static penetration tests. The basic equation of pressure-sinkage relationship is given by

$$p = (k_c/B + k_\phi)z^n. \tag{1}$$

Therein $p$ is the pressure in the contact patch, $z$ the tyre sinkage, $k_c$ the cohesion module, $k_\phi$ the friction module of soil, $n$ the sinkage exponent and $B$ the width of the tyre contact patch (see also Fig. 1). Multibody system simulation gives the opportunity of dynamic simulations and makes it necessary to extend Eq. (1) of Bekker so that dynamic effects in the wheel soil contact patch are considered properly in the simulation scenario. Therefore the rheological soil model is introduced (see Fig. 5).

Important characteristics of planetary rovers are the multi-axle suspension and an all-wheel drive. Therefore the multipass-effect with the rheological soil model and, for driven and braked wheels, the wheel slip on soft soil has to be taken into account. Tractive efficiency is an important value to evaluate mobility and can be expressed by

$$F_d = F - R \tag{2}$$

where the drawbar pull $F_d$ is equal to the difference of the tractive effort $F$ and the resulting resistance force $R$.

The drawbar pull can also be defined by the difference between soil thrust and motion resistance and is the force which is available to pull or push another vehicle until the maximum available traction is reached. The various complex effects encountered in terramechanics are described in the following.


## Wheel slip on soft soil

Wheels of currently designed NASA Mars rovers do not have any pneumatic tyres and therefore can be assumed to be rigid wheels, which is quite a good assumption for pneumatic wheels as well, because the soil deformation is much greater than the tyre deflection [4]. However, more advanced designs try to take into account the advantages of elastically designed wheels. In Fig. 1 the correlation of a rolling rigid wheel and the sinkage on soft soil is shown [5]. Therein $F_{Z,W}$ is the tyre load, $F_{X,W}$ the rolling drag, $z_0$ the tyre sinkage and $\dot{\theta}_w$ the angular velocity of the wheel. The angle $\theta_0$ defines the angle between the tyre contact patch and the first contact point of the rolling tyre and the undeformed terrain. The longitudinal wheel slip $S_{X,W}$ has to be taken into account when considering driven or braked wheels. The definition in Eqs. (3) and (4) of longitudinal slip $S_{X,W}$ is different for accelerating ($S_{X,W,A}$) and decelerating ($S_{X,W,D}$) wheels:

$$S_{X,W,A} = \frac{r\dot{\theta}_w - v_w}{r\dot{\theta}_w} \tag{3}$$

$$S_{X,W,D} = \frac{v_w - r\dot{\theta}_w}{v_w} \tag{4}$$

To make things easier for the following equations this case differentiation for longitudinal slip definition will be introduced

$$i = \begin{cases} \frac{r\dot{\theta}_w - v_w}{r\dot{\theta}_w} & r\dot{\theta} > v_w \text{ accelerating mode} \\ \frac{v_w - r\dot{\theta}_w}{v_w} & r\dot{\theta} < v_w \text{ decelerating mode} \end{cases} \tag{5}$$

Therein $r$ is the wheel radius, $\dot{\theta}_w$ the wheel angular velocity and $v_w$ the translational wheel velocity. To describe the difference of longitudinal slip characteristics on rigid and soft grounds Fig. 3 is introduced. In Fig. 3 the slip curves of a tyre rolling on rigid and soft soil surface are compared with the slip $S_{X,W}$ on the abscissa and the friction coefficient $\mu$ on the ordinate. The curve on soft soil is strongly dependent on the used soil type but generally does not have the characteristic peak of the slip curves on rigid surfaces. The peak defines the transition from nearly pure rolling to combined rolling and sliding of the tyre. Total sliding is reached when the slip $S_{X,W} = 1$ which holds for acceleration and deceleration case. This definition of $S_{X,W}$ takes values between 0 and 1.

Wheel slip characteristics on soft soil differs from slip on rigid ground as shown in the example of Fig. 3 and described by [2]. In particular the magnitude of slip on soft soil for the same tractive effort is mostly much higher than that on rigid ground and is furthermore dependent on the shear stress maximum $\tau_{max}$ of the soil that can be gained from Eq. (13). With the notations of Fig. 1 and Fig. 2 the slip velocity $v_j$ can be given by Eq. (11) and this leads to the shear displacement $j$ in the wheel-soil contact patch given in Eq. (12). With the relationship between shear stress and shear displacement one can obtain the shear stress distribution $\tau(\theta)$ given in Eq. (13).

*9th ESA Workshop on Advanced Space Technologies for Robotics and Automation ASTRA 2006*
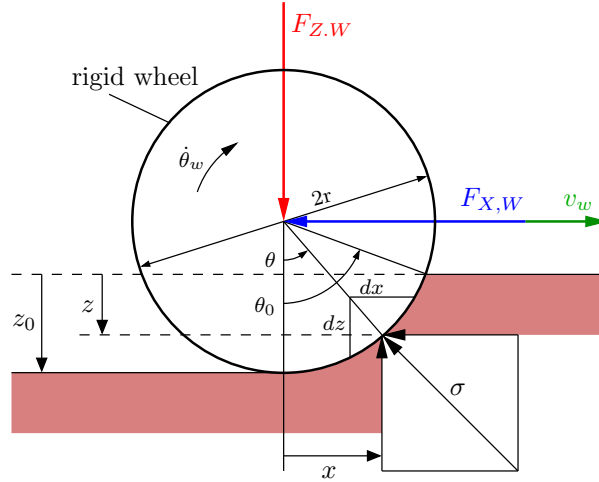*28-30 November 2006 at ESTEC, Noordwijk, the Netherlands*

2

Fig. 1: Correlation of a rigid wheel on soft soil illustrating the forces acting on the wheel and the geometry in the tyre-soil contact patch

In Fig. 2 the correlation for the value of $v_w t$ and $v_r$ in point $P$ of the rigid wheel is shown. With the slip definition of Eq.6 one gets the translational wheel velocity $v_w$ in Eq. 7.

$$i \;=\; 1 - \frac{v_w}{r\dot{\theta}_w} \tag{6}$$

$$v_w \;=\; (1-i)r\dot{\theta}_w \tag{7}$$

$$v_{wt} \;=\; v_w \cos\theta \tag{8}$$

$$v_{wr} \;=\; r\dot{\theta}_w \tag{9}$$

With the sum of the tangential velocities of point $P$ in Fig. 2 one gets:

$$v_j = v_r - v_{wt} \tag{10}$$

With these equations one gets the slip velocity by:

$$v_j = r\dot{\theta}_w \left[1 - (1-i)\cos\theta\right] \tag{11}$$

the shear displacement $j$ by:

$$j = \int_0^{\theta_0} r\dot{\theta}_w \left[1 - (1-i)\cos\theta\right] \frac{d\theta}{\theta_w} \tag{12}$$

and the shear stress $\tau(\theta)$ by:

$$\tau(\theta) = \left[c + p(\theta)\tan\phi\right]\left(1 - e^{-j/k}\right) \tag{13}$$

Therein $\dot{\theta}_w$ is the wheel angular velocity and $i = S_{X,W}$ the longitudinal wheel slip as defined by Eqs. (3) and (4) (see Fig. 2). The used soil parameters are the cohesion $c$, a soil modulus $k$ and the angle of internal shearing resistance $\phi$.

The integration of the horizontal component of Eq. 13 leads to the total tractive effort $F$

$$F = rb \int_0^{\theta_0} \tau(\theta)\cos\theta \, d\theta \tag{14}$$

When taking into account the vertical shear stress component for the wheel load $F_z$ in contrast to the simplified wheel contact model of Fig. 1 one gets the following equations for vertical load $F_z$, drawbar pull $F_d$ and wheel
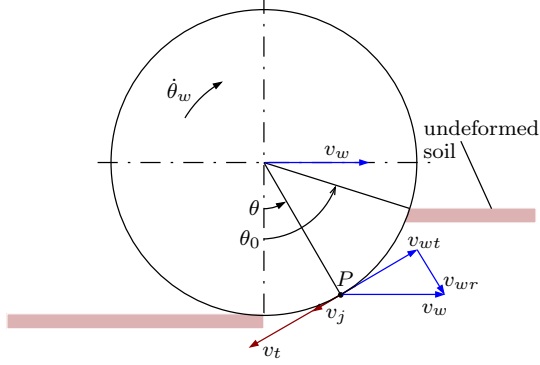
Fig. 2: Slip velocity $v_j$ of a rigid wheel without grousers rolling with slip due to a driving torque on soft soil which leads to the shear displacement $j$ in the range of the contact patch with the arc length $\theta_0$
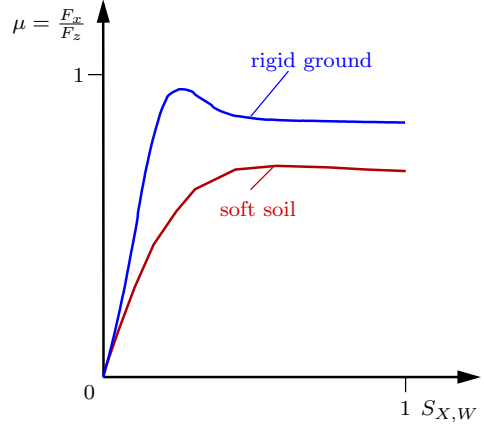


Fig. 3: Comparison of slip $S_{X,W}$ versus friction coefficient $\mu$ of a rigid and a soft soil surface

torque $M_\omega$:

$$F_z = rb \left[ \int_0^{\theta_0} p(\theta) \cos \theta d\theta + \int_0^{\theta_0} \tau(\theta) \sin \theta d\theta \right] \tag{15}$$

$$F_d = rb \left[ \int_0^{\theta_0} \tau(\theta) \cos \theta d\theta - \int_0^{\theta_0} p(\theta) \sin \theta d\theta \right] \tag{16}$$

$$M_\omega = r^2 b \int_0^{\theta_0} \tau(\theta) d\theta \tag{17}$$

## Rheological soil model - dynamical contact model

Investigations by Bolling [6] led to a rheological soil contact model with elasto-plastic behaviour. The elastic behaviour of the soil is especially important for multipass manoeuvres because it affects the soil conditions for the wheels rolling behind each other (compare with Fig. 4). The diagram shown in Fig. 5 depicts the schematic mechanical system with the elastic (stiffness $c_f$ and Newtonian viscosity $\eta$) and plastic (compression $\mu_v$ and yielding constant $\mu_p$) part of the rheological soil model which in addition to the approaches of Bekker and Wong [2, 3] takes into account the sinkage velocity $\dot{z}$. Corresponding to Eq. (1) the equations for the pressure-sinkage relationship are given by:

$$p_{dyn} = c_f(z_{el} - z_{pl}) + \eta(\dot{z}_{el} - \dot{z}_{pl}) \tag{18}$$
$$p_{dyn} = \mu_v z_{pl} + \mu_p \tag{19}$$

Eq. (18) describes the equilibrium of forces of the elastic part and Eq. 19 represents the equilibrium of forces of the plastic part of the soil deformation with the dynamical soil pressure $p_{dyn}$.

The time derivative of Eq. (19)

$$\dot{p}_{dyn} = \mu_v \dot{z}_{pl} \tag{20}$$

and insertion of Eq. (19) and Eq. (20) into Eq. 18 leads to

$$\dot{p}_{dyn} + \frac{c_f + \mu_v}{\eta} p_{dyn} = \mu_v \dot{z}_{el} + \frac{c_f \mu_v}{\eta} z_{el} + \frac{c_f \mu_p}{\eta} \tag{21}$$
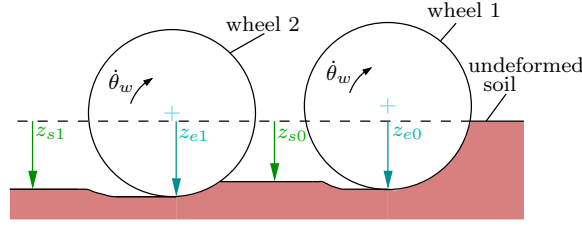
*9th ESA Workshop on Advanced Space Technologies for Robotics and Automation ASTRA 2006*
*28-30 November 2006 at ESTEC, Noordwijk, the Netherlands*

4

Fig. 4: Difference between tyre sinkage $z_{ei}$ and rut depth $z_{si}$ on multi-axle vehicles

Therein $z_{el}$ and $z_{pl}$ are the sinkages of the elastic and plastic part, $c_f$ is a stiffness parameter and $\eta$ the Newtonian viscosity. In the plastic part of the model $\mu_p$ and $\mu_v$ are the yielding and compression constant. When solving the differential equation (20) one obtains the pressure-sinkage relationship of the rheological soil model in

$$p_{dyn} = [(\frac{\mu_v}{c_f + \mu_v})^2 \eta \dot{z} + \frac{c_f \mu_p}{c_f + \mu_v}][1 - e^{\frac{c_f + \mu_v}{\eta v} z}] + \frac{c_f \mu_v}{c_f + \mu_v} z \qquad (22)$$

which makes up for Bekker's pressure-sinkage relation in Eq. (1). Therefore the following assumptions are made:

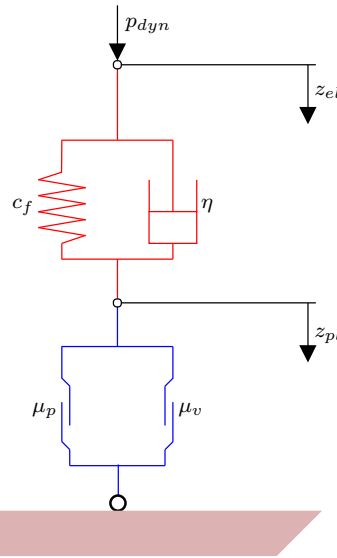$$\dot{z}_{el} = \dot{z} \qquad (23)$$
$$z_{el} = z \qquad (24)$$



Fig. 5: Schematic illustration of the rheological soil contact model representing the elastic (red) and plastic (blue) properties of the soil [6]

The parameters needed for the rheological soil model can be adopted from measurable parameters like the ones listed in [7] gained from simulated Martian soil under laboratory conditions. This gives an opportunity to use soil measurement made on earth and build up a MBS simulation environment that represents the rover's behaviour in its Martian environment.

**WHEEL-SOIL INTERFACE TO MBS ENVIRONMENT**

The wheel-soil interaction is implemented as tyre force user routine in SIMPACK. Therefore a standard tyre interface in SIMPACK can be used which is a good choice to build up a modular model structure that is not bound to a specific MBS code. The tyre interface is compatible to the Standard Tyre Interface (STI) and

Tyre Data Exchange (TYDEX) format, as described by Oosten et al. [8], which makes it possible to migrate the simulation environment to other MBS codes or simulation tools which are compatible to these widely used standardisations. Furthermore the modular concept makes it possible to integrate in particular control elements into the simulation environment like the slip based traction control by Yoshida et al. [9]. The advantages of using the SIMPACK user tyre interface are especially the integrated slip calculations and road evaluations. Furthermore all relative transformations between inertia-frame, road-obstacle frames tyre-frames on the road-tangential plane, the tyre-carrier frame and the tyre centre frame are available in the user tyre module.

Finally the dynamic multibody simulation can be exported to VRML format so that the rover can be animated with an impression of Martian environment as shown in the example in Fig. 6 which depicts the rover assembled with its complete CAD data simulated in SIMPACK and coping with Martian obstacles. Step simulation for obstacles is not possible so far so that obstacles must have a continuous shape in first and second approximation. This gives the opportunity to combine visualisation tools with a dynamical model based on physical properties of the tyre-soil interaction.
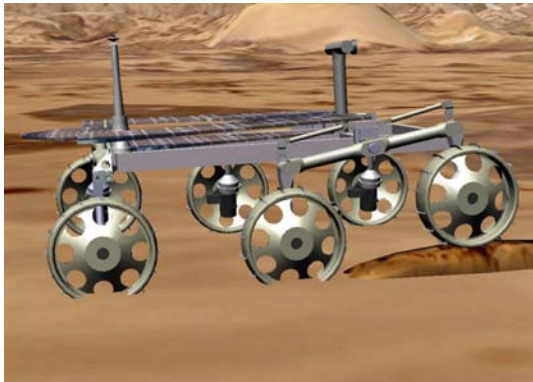


Fig. 6: Animated SIMPACK 3D Multibody System model with integrated CAD data of the rover converted to VRML format in Martian environment
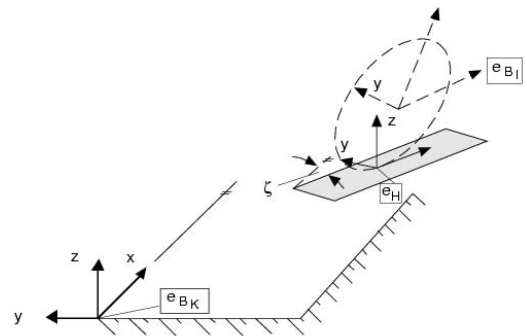


Fig. 7: Tyre coordinate system $e_H$ on the road

## TPM INTEGRATION - VALIDATION

In the frame of the ESA Rover Chassis Evaluation Tool (RCET) the Tractive Prediction Module (TPM) has been developed and validated [10]. The aim was now to integrate the TPM into the MBS environment. Therefore the SIMPACK user force element is used which calculates the vertical contact force $F_z$ and the driving torque $M_y$. By means of these values and typical wheel and soil parameters the TPM calculates the output values for wheel sinkage, rolling resistance, etc.

With the coupling of the TPM and the rheological soil model into the SIMPACK model environment validated, dynamic simulation scenarios are possible.

The TYDEX standard is used in the user tyre routine and so are the additional terrain parameters integrated into the TYDEX input file.

## DISCUSSION OF RESULTS

Simulation results are shown comparing the standalone TPM executed within the command line and the integration in the Simpack MBS environment. An example output of the TPM with the wheel load $F_z$ and wheel torque $M_y$ as input parameters is shown:

The output of the TPM is ASCII text only and for further processing the results are save semicolon separated.

First simulation results with the TPM integrated into the Simpack environment are presented. Therefore the wheel is put onto the ground and the gradient shown in Fig. 8 for the wheel load $F_z$ is gained as input value

for the terramechanical calculation. As for the standalone TPM calculation the drive torque is constant at $T_y = 2$ Nm
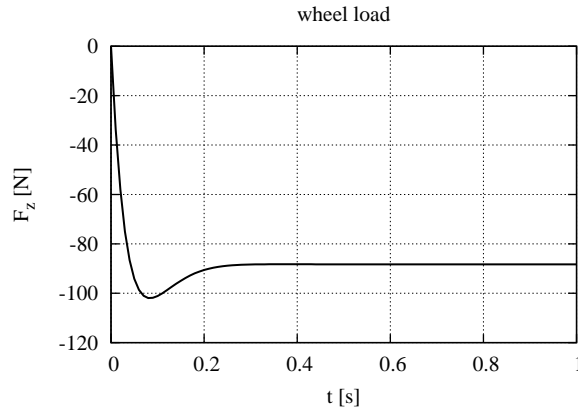


Fig. 8: Wheel load with simple contact force implementation

The magnitude of the load sinkage $z_w$ in Fig. 9 confirms well with the standalone TPM. The static value reaches $z_w = 35.5$ mm for the specified load.

The value of the grousers in contact differs from the standalone TPM. This part of the module has to be adapted further to fulfil the needs of the time integration of the multibody formalism. But this value does not influence the further multibody calculations.
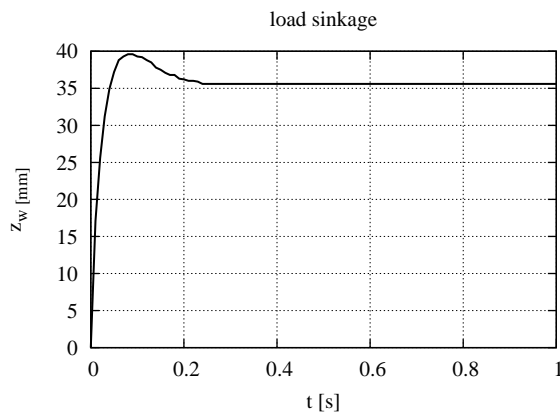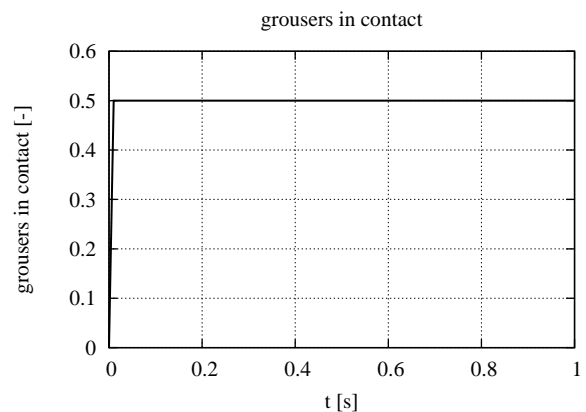


Fig. 9: Load sinkage $z_w$



Fig. 10: Grousers in contact

The rolling resistance $R$ of the driven wheel shown in Fig. 11 confirms well with the static calculations. The drawbar pull $DP$ calculation differs as well from the TPM stand alone calculation.

**REFERENCES**

[1] A. Gibbesch and B. Schäfer. Modelling of planetary rovers by means of a dynamical system approach with respect to mobility requirements. In *The 10th European Conference of the ISTVS 2006*, Budapest, Hungary, 3-6 October 2006.
[2] J. Y. Wong. *Theory of Ground Vehicles.* Wiley, New York, 3. edition, 2001.
[3] M. G. Bekker. *Introduction to Terrain-Vehicle Systems.* The University of Michigan Press, Ann Arbor, 1969.
[4] S. A. Shoop. *Finite Element Modeling of Tire-Terrain Interaction.* PhD thesis, University of Michigan, Ann Arbor, 2001.
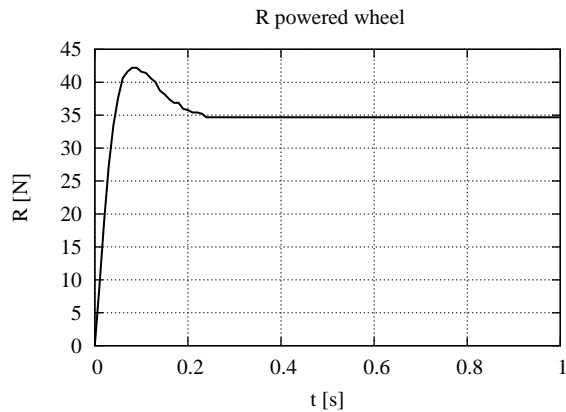
*9th ESA Workshop on Advanced Space Technologies for Robotics and Automation ASTRA 2006*
*28-30 November 2006 at ESTEC, Noordwijk, the Netherlands*
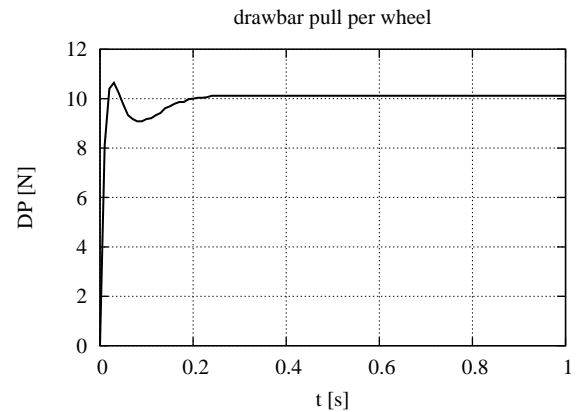
7

Fig. 11: $R$ powered wheel



Fig. 12: Drawbar pull per wheel

[5] M. G. Bekker. *Theory of Land Locomotion.* The University of Michigan Press, Ann Arbor, 2. edition, 1962.

[6] I. Bolling. *Bodenverdichtung und Triebkraftverhalten bei Reifen - Neue Meß- und Rechenmethoden.* Dissertation, TU München, 1987.

[7] L. Richter, M. C. Bernasconi, and P. Coste. Analysis, design and test of wheels for a 4kg class mobile device for the surface of mars. In *14th International Conference of the International Society for Terrain-Vehicle Systems*, Vicksburg, MS USA, October 2002.

[8] J. van Oosten, H.-J. Unrau, A. Riedel, and E. Bakker. Tydex workshop: Standardisation of data exchange in tyre testing and tyre modelling. In F. Böhm and H.-P. Willumeit, editors, *Proceedings of the 2nd International Colloquium on Tyre Models for Vehicle Dynamic Analysis, held at the Technical University of Berlin, Germany, February 20-21, 1997*, volume 27 of *Supplement to Vehicle System Dynamics*, pages 272–288, Lisse, 1997. Swets & Zeitlinger.

[9] K. Yoshida, H. Hamano, and T. Watanabe. Slip-based traction control of a planetary rover. In *8th International Symposium on Experimental Robotics, ISER 2002*, Sant'Angelo d'Ischia, Italy, 2002.

[10] L. Richter, A. Ellery, Y. Gao, S. Michaud, N. Schmitz, and S. Weiß. A Predictive Wheel-Soil Interaction Model for Planetary Rovers Validated in Testbeds and Against MER Mars Rover Performance Data. In *The 10th European Conference of the ISTVS 2006*, Budapest, Hungary, 3-6 October 2006.

*9th ESA Workshop on Advanced Space Technologies for Robotics and Automation ASTRA 2006*
*28-30 November 2006 at ESTEC, Noordwijk, the Netherlands*

8